INTERNATIONAL JOURNAL FOR NUMERICAL METHODS IN FLUIDS
Int. J. Numer. Meth. Fluids 2010; **62**:428–448
Published online 2 April 2009 in Wiley InterScience (www.interscience.wiley.com). DOI: 10.1002/fld.2027

Well-balancing issues related to the RKDG2 scheme for the shallow water equations

Georges Kesserwani[1, 2, *, †], Qiuhua Liang[1], José Vazquez[2] and Robert Mosé[2]

[1]*School of Civil Engineering and Geosciences, Newcastle University, Newcastle upon Tyne NE1 7RU, U.K.*
[2]*U.P.R. Systèmes Hydrauliques Urbains, Ecole Nationale du Génie de l'Eau et de l'Environnement de Strasbourg, 1 quai Koch-BP 61039, 67070 Strasbourg Cedex, France*

SUMMARY

Discontinuous Galerkin (DG) finite element methods have salient features that are mainly highlighted by their locality, their easiness in balancing the flux and source term gradients and their component-wise structure. In the light of this, this paper aims to provide insights into the well-balancing property of a second-order Runge–Kutta Discontinuous Galerkin (RKDG2) method. For this purpose, a Godunov-type RKDG2 method is presented for solving the shallow water equations. The scheme is based on local DG linear approximations and does not entail any special treatment of the source terms in order to achieve well-balanced numerical results. The performance of the present RKDG2 scheme in reproducing conserved solutions for both free surface and discharge over strongly irregular topography is demonstrated by applying to several hydraulic benchmarks. Meanwhile, the effects of different slope limiting procedures on the well-balancing property are investigated and discussed. This work may provide useful guidelines for developing a well-balanced RKDG2 numerical scheme for shallow water flow simulation. Copyright © 2009 John Wiley & Sons, Ltd.

Received 14 May 2008; Revised 3 February 2009; Accepted 4 February 2009

KEY WORDS: Saint Venant equations; Godunov-type scheme; discontinuous Galerkin finite element method; slope limiting; irregular topography; C-property; local linear approximations; source terms

1. INTRODUCTION

Shallow water equations have a wide range of applications in describing one- or two-dimensional free surface flow hydrodynamics in artificial channels, natural rivers, coastal areas, etc. A large number of numerical schemes and computational techniques have been reported in the literature

*Correspondence to: Georges Kesserwani, School of Civil Engineering and Geosciences, Newcastle University, Newcastle upon Tyne NE1 7RU, U.K.
†E-mail: Georges.Kesserwani@newcastle.ac.uk

Contract/grant sponsor: UK Engineering and Physical Sciences Research Council (EPSRC); contract/grant number: EP/F030177/1

for solving these equations using finite difference, finite volume or finite element methods [1–5]. During the past two decades, Godunov-type schemes [1, 6] have become popular in solving the hyperbolic conservation laws that consists of the shallow water equations owing to their superior advantage of automatic shock-capturing. A finite volume Godunov-type scheme solves the integral form of the governing equations at the discrete level with the computational domain decomposed onto a grid. The flow data are normally stored at the cell centres, representing the local averages of flow variables over an entire cell. The cell-centred flow variables are updated in time by correctly balancing the interface fluxes that are approximated by the Riemann solutions [7]. Thus, efficient and accurate computation of fluxes across cell interfaces is crucial for a high-order finite volume scheme. As the flow data are only available at the cell centres, accurate point values of the flow variables at the cell interface must be reconstructed from the neighbouring cell-centred information in order to obtain a high-order approximation. These face values are then used to calculate interface fluxes by solving local Riemann problems. This process may be defined as local if it only involves the flow information from the direct neighbouring cells. The simplest finite volume model would be the one based on a three-point scheme that requires than information from the cell under consideration and its two direct neighbours. However, any three-point Total Variation Diminishing (TVD) scheme is at most first-order accurate [5]. To achieve second-order accuracy under the TVD condition, at least a five-point stencil scheme must be employed [2].

To reach the desirable high-order accuracy without using a reconstruction procedure, Discontinuous Galerkin (DG) approximating polynomials are of great interest. A DG spatial framework starts with the local averages of flow information together with their corresponding local (natural) high-order slopes on a three-cell scheme. Even for simulations involving locally steep gradients of the flow variables that require a slope limiting process, computation is at most performed on a five-cell stencil [8]. DG methods, therefore, provide an attractive alternative and probably a more efficient way for solving the shallow water equations or the so-called Saint Venant equations. For time-dependant problems, the usual strategy is first to apply a DG scheme to discretize the governing equations in space and then to employ an appropriate time integration method to march the flow variables to a new time step. A particularly powerful choice is to combine a DG approach with a Runge–Kutta (RK) time integration method [9], which is termed RK Discontinuous Galerkin (RKDG) scheme (refer to [10] for a fundamental background). RKDG methods boast about their advantages in locality, Godunov-type features, adaptivity in polynomial order, conservation properties, and many others [10–14].

In recent years, shallow water equations have been increasingly used in real-world river modelling and flood simulations, where the domain topographies are normally very complex (e.g. mountainous areas, abruptly varying river banks, rural and urban floodplains). It is well-known that a numerical scheme should be well balanced, i.e. preserve the solution of a lake at rest at the discrete level [15–19], in order to obtain sensible solutions for problems involving irregular bed profiles. Constructing a well-balanced scheme for predicting flow hydrodynamics over highly complicated domain topographies, especially in the context of Godunov-type methods [6], is still a challenging issue receiving intensive attentions from scientific researchers and hydraulic modelers. In an early paper, Roe [20] indicated that a pointwise evaluation of the source terms is not a suitable strategy for constructing a well-balanced scheme. Now the necessity of an upwind discretization of the source terms is widely recognized [21–25] and reliable numerical simulations can only be obtained from numerical schemes that balance the flux and source term gradients.

In developing a well-balanced scheme for shallow water flows, Bermúdez and Vázquez-Cendón [21] proposed an upwind method to handle the bed slope source terms using the Q-scheme of van

DOI: 10.1002/fld

Leer and Roe [21] and defined the so-called *C-property* (*C* stands for Conservation). A scheme satisfying the *C-property* prevents the propagation of parasitic waves in steady and quasi-steady flows. Such a scheme is also referred to as well-balanced by Greenberg and LeRoux [26] and later many other investigators [3, 18, 19, 27, 28]. The upwind treatment of source terms has been adopted and improved for achieving well-balanced schemes by many other researchers. Vázquez-Cendón [25] investigated further the upwind method for discretizing the source terms and widened the range of applications for more complex problems. LeVeque [16] developed a high-resolution method for balancing the flux and source term gradients that provides accurate solutions for quasi-steady problems. But the method faces difficulty when simulating steady transcritical flow with shocks. Hubbard and García-Navarro [29] extended the upwind philosophy of Bermúdez and Vázquez-Cendón [21] and presented a well-balanced high-resolution MUSCL scheme. The scheme is able to handle steady and unsteady transcritical flows with shocks. Črnjarić-Žic *et al*. [22] proposed a well-balanced high-order finite volume upwind WENO schemes for the open-channel flow problems. Crossely and Wright [23] combined the local time stepping techniques and the upwind treatment of source terms to achieve well-balancing. Yet, source term upwinding is not straightforward for the high-order RKDG methods due to the necessity of dealing with high-order approximations of the source term integrals [8].

Other techniques have also been reported in the literature to achieve a well-balanced scheme. Zhou *et al*. [30, 31] initiated a simple surface gradient method (SGM) within the MUSCL-Hancock scheme. The ground of the method is to consider the formulation of the shallow water equations with the flux vectors evaluated in term of the surface gradient variable. This renders a mathematically well-balanced system without any need of special treatment for the source terms [3, 32]. The SGM can be used in any high-resolution Godunov-type scheme that requires data reconstruction and was latterly applied by Tseng [33, 34] to improve the performance of many renowned traditional high-resolution TVD methods and by Caleffi *et al*. [35] to build a high-order well-balanced central WENO scheme. Recently, Xing and Shu [36] presented a more general approach to the SGM and applied it to furnish a class of high-order finite volume WENO schemes and finite element RKDG methods with the well-balanced property. The key ingredient of the approach is a proper decomposition of the source terms that ensures the well-balancing and preserves the genuinely high-accuracy of the methods. However, the drawback of this method is its complexity, which was also acknowledged by the authors in their recent paper [37]. The SGM was also considered by Aureli *et al.* [28] to build a weighted SGM in the framework of the SLIC scheme [5]. The method computes water depth at the cell boundaries through a weighted average of the extrapolated values deriving from depth gradient method and SGM reconstruction. In the approach of Audusse *et al*. [27], another technique called hydrostatic reconstruction was introduced for achieving well-balancing in the context of a finite volume Godunov-type method. The extension of this method to very high-order accurate schemes is described by Noelle *et al*. [18]. Xing and Shu [37], based on a generalization of the method due to Audusse *et al.* [27] and Noelle *et al.* [18], established a group of easier approaches for constructing well-balanced RKDG and WENO schemes by allowing more freedom in defining the approximate polynomials. The enhanced approaches require less computational efforts, at least for the RKDG methods.

This work discusses in depth the well-balancing issues in the context of a second-order RKDG scheme (RKDG2) for numerically solving the Saint Venant equations. A three-cell well-balanced RKDG2 scheme is first presented. The difference between the proposed numerical scheme and any other second-order finite volume method is that the local linear approximation is based on a local well-balanced hypothesis, which leads to a natural well-balanced scheme for both water

DOI: 10.1002/fld

surface elevation and discharge without any need for special treatment of the source terms. The well-balanced local RKDG2 scheme is extended to wider applications by incorporating with a slope limiting procedure and the effects of different slope limiting procedures on the well-balancing property are investigated and discussed in the context of numerical tests. The paper is organized as follows. Following in Section 2, the governing shallow water equations are introduced. Section 3 details the well-balanced local RKDG2 numerical scheme and the slope limiting procedure for more general simulations. In Section 4, the performance of local RKDG2 scheme is validated against a number of numerical benchmark tests and the effects of different slope limiting procedures are also discussed. At last, brief concluding remarks are drawn in Section 5 to complete the work.

2. SHALLOW WATER EQUATIONS

Situations in fluid dynamics where the horizontal length scale is much greater than the vertical extent are common in real-life applications, e.g. flow over a floodplain or along a wide channel reach. In these cases, the 3D Navier–Stokes equations that describe the flow dynamics may be depth-averaged and simplified to become the 2D shallow water system. When modelling flow hydrodynamics in long rivers and artificial channels, the dimensionality of 2D shallow water equations may be further reduced to one, which leads to the 1D nonlinear shallow water equations. The conservative form of the Saint Venant equations written in term of water depth h (m) and unit-width discharge q (m^2/s) is given by

$$\begin{aligned} h_t + q_x &= 0 \\ q_t + (q^2/h + gh^2/2)_x &= ghS_0 \end{aligned} \tag{1}$$

where x denotes the space coordinate, t represents time, g is the gravity acceleration, $S_0(x) = -\partial z/\partial x$ is the bed slope term (or bed gradient) with $z(x)$ being the channel bottom elevation. The above governing partial differential equations (PDEs) may be also written in a matrix form as

$$\mathbf{U}_t + \mathbf{F}_x = \mathbf{S} \tag{2}$$

where $\mathbf{U} = [h, q]^{\mathrm{T}}$ is designated as the vector of conserved flow variables, $\mathbf{F} = [q, q^2/h + gh^2/2]^{\mathrm{T}}$ is the flux vector, $\mathbf{S} = [0, ghS_0]^{\mathrm{T}}$ is the vector containing the source terms.

Employing the flux Jacobian matrix ($\mathbf{J} = \partial\mathbf{F}/\partial\mathbf{U}$) with respect to the flow variable vector, Equation (2) can be also expressed in a quasi-linear form

$$\mathbf{U}_t + \mathbf{J}\mathbf{U}_x = \mathbf{S} \tag{3}$$

Herein $\mathbf{J}$ has two real eigenvalues $\lambda^{1,2} = u \pm c$ where u is the velocity (inertia effects) and $c = \sqrt{gh}$ is the wave celerity (gravitational effects). The two eigenvalues are real and distinct when $h > 0$, which indicates the hyperbolicity of the governing equations. The corresponding independent and real eigenvectors are given by $\mathbf{e}^{1,2} = [1, \lambda^{1,2}]^{\mathrm{T}}$.

3. WELL-BALANCED RKDG2 METHOD

Godunov-type upwind schemes [1, 6] are one of the most accurate group of numerical methods for solving the nonlinear hyperbolic equations. In this section, we first detail a Godunov-type

DOI: 10.1002/fld

scheme based on local finite element DG linear approximations. The scheme naturally achieves the well-balanced property without necessity for any special treatment of the bed slope source term. Then a slope-limiting procedure is briefly described to extend the local scheme to more severe flow simulations.

3.1. A review of the RKDG2 scheme

The computational domain is divided into N cells with cell i defined as $I_i=[x_{i-1/2}; x_{i+1/2}]$, where $0=x_{1/2}<x_{3/2}<\cdots<x_{N+1/2}=L$ are the boundary points and $x_i=(x_{i+1/2}+x_{i-1/2})/2$ is the cell centre. The cells are assumed to be uniform, of size $\Delta x=x_{i+1/2}-x_{i-1/2}$. A local linear approximation $\mathbf{U}_h=[h_h(x,t), q_h(x,t)]^{\mathrm{T}}$ to $\mathbf{U}(x,t)$ belonging to the finite-dimensional space $P^1(I_i)$ [10] is used to achieve second-order spatial accuracy.

Similar to the traditional finite element method, the PDE system (2) is weighted by a continuous test function v_h and integrated locally over I_i to give

$$\int_{I_i} \partial_t \mathbf{U}_h(x,t) v_h(x)\,\mathrm{d}x + \int_{I_i} \partial x \mathbf{F}(\mathbf{U_h}(x,t)) v_h(x)\,\mathrm{d}x = \int_{I_i} \mathbf{S}(\mathbf{U_h}(x,t), S_0(x)) v_h(x)\,\mathrm{d}x \tag{4}$$

Integration by part to the flux derivative terms gives the following weak formulation:

$$\int_{I_i} \partial_t \mathbf{U_h}(x,t) v_h(x)\,\mathrm{d}x + \Big[\mathbf{F}(\mathbf{U_h}(x_{i+1/2},t)) v_h(x_{i+1/2}) - \mathbf{F}(\mathbf{U_h}(x_{i-1/2},t)) v_h(x_{i-1/2}) - \int_{I_i} \mathbf{F}(\mathbf{U_h}(x,t)) v_h(x)\,\mathrm{d}x\Big] = \int_{I_i} \mathbf{S}(\mathbf{U_h}(x,t), S_0(x)) v_h\,\mathrm{d}x \tag{5}$$

The system (5) is decoupled by adopting the Legendre polynomial as a local basis function [10].

In each cell, the local approximate linear solution $\mathbf{U_h}(x,t)$ is generated by an average value of flow variables $\mathbf{U}_i^0(t)$ and a slope value $\mathbf{U}_i^1(t)$ as

$$\mathbf{U_h}(x,t)\rfloor_{I_i} = \mathbf{U}_i^0(t) + 2\mathbf{U}_i^1(t)(x-x_i)/\Delta x \quad (\forall x \in I_i) \tag{6}$$

where $\{\mathbf{U}_i^0(t), \mathbf{U}_i^1(t)\}$ are, in the context of a finite element framework, the degrees of freedom that should be stored and evolved locally in each cell over time starting from the compatible projection of the initial conditions $\mathbf{U}_0(x)=\mathbf{U}(x,0)$,

$$\begin{aligned} \mathbf{U}_i^0(0) &= (\mathbf{U}_0(x_{i+1/2}) + \mathbf{U}_0(x_{i-1/2}))/2 \\ \mathbf{U}_i^1(0) &= (\mathbf{U}_0(x_{i+1/2}) - \mathbf{U}_0(x_{i-1/2}))/2 \end{aligned} \tag{7}$$

The local initial data $P^1(I_i)$-projection to give the above initial conditions will be discussed in details in Section 3.2.

After assigning the initial data, the next step is to evaluate the spatial update of $\mathrm{d}\mathbf{U}_i^{0,1}/\mathrm{d}t$,

$$\mathrm{d}\mathbf{U}_i^{0,1}/\mathrm{d}t = \mathbf{L}_i^{0,1}(\mathbf{U}_{i-1}^{0,1}, \mathbf{U}_i^{0,1}, \mathbf{U}_{i+1}^{0,1}) \tag{8}$$

where $\mathbf{L}_i^{0,1}$ are the DG operators for spatially approximating the time derivative of the degrees of freedoms $\mathbf{U}_i^{0,1}$. The operators require, in principle, information from three cells. However, as

DOI: 10.1002/fld

it will be discussed in Section 3.3, more cells will be involved when performing a slope limiting procedure. The final forms of the spatial operators are,

$$\mathbf{L}_i^0 = -\frac{1}{\Delta x}[\tilde{\mathbf{F}}_{i+1/2} - \tilde{\mathbf{F}}_{i-1/2} - \Delta x \mathbf{S}(\mathbf{U}_i^0, S_0)] \tag{9}$$

$$\mathbf{L}_i^1 = -\frac{3}{\Delta x}\left\{\begin{array}{l}\tilde{\mathbf{F}}_{i+1/2} + \tilde{\mathbf{F}}_{i-1/2} - \mathbf{F}(\mathbf{U}_i^0 + \mathbf{U}_i^1/\sqrt{3}) - \mathbf{F}(\mathbf{U}_i^0 - \mathbf{U}_i^1/\sqrt{3}) \\ \quad -\Delta x\sqrt{3}/6[\mathbf{S}(\mathbf{U}_i^0 + \mathbf{U}_i^1/\sqrt{3}, S_0) - \mathbf{S}(\mathbf{U}_i^0 - \mathbf{U}_i^1/\sqrt{3}, S_0)]\end{array}\right\} \tag{10}$$

where $\tilde{\mathbf{F}}_{i\pm1/2}$ are the numerical fluxes across the positive and negative cell interfaces resulting from solutions of the local Riemann problems, which are estimated using the approximate Riemann solver of Roe [20, 38]. For example, the fluxes $\tilde{\mathbf{F}}_{i+1/2}$ through the cell interface $i+1/2$ can be computed by (similar formulae can be obtained for fluxes through other cell interfaces)

$$\tilde{\mathbf{F}}_{i+1/2} = \tilde{\mathbf{F}}(\mathbf{U}_{i+1/2}^-, \mathbf{U}_{i+1/2}^+) = \frac{1}{2}\left[\mathbf{U}_{i+1/2}^- + \mathbf{U}_{i+1/2}^+ - \sum_{p=1}^{2} \alpha_{i+1/2}^p |\tilde{\lambda}_{i+1/2}^p| \tilde{\mathbf{e}}_{i+1/2}^p\right] \tag{11}$$

Together with a local adjustment of the intermediate eigenvalues,

$$|\tilde{\lambda}_{i+1/2}^p|^* = \begin{cases} |\tilde{\lambda}_{i+1/2}^p| & \text{if } |\tilde{\lambda}_{i+1/2}^p| \geqslant \varepsilon^p \\ (\tilde{\lambda}_{i+1/2}^p)^2/2\varepsilon^p + \varepsilon^p/2 & \text{if } |\tilde{\lambda}_{i+1/2}^p| < \varepsilon^p \end{cases} \tag{12}$$

where

$$\varepsilon^p = \min(\tilde{c}_{i+1/2}, \max(0, 2(\lambda_{i+1/2}^{+,p} - \lambda_{i+1/2}^{-,p}))) \tag{13}$$

Then a two step RK method is adopted to achieve second-order accuracy in time,

$$(\mathbf{U}_i^{0,1})^{n+1/2} = (\mathbf{U}_i^{0,1})^n + \Delta t\,(\mathbf{L}_i^{0,1})^n \tag{14}$$

$$(\mathbf{U}_i^{0,1})^{n+1} = [(\mathbf{U}_i^{0,1})^n + (\mathbf{U}_i^{0,1})^{n+1/2} + \Delta t\,(\mathbf{L}_i^{0,1})^{n+1/2}]/2 \tag{15}$$

It is worth pointing out that the stability of the aforementioned explicit RKDG2 scheme is controlled by the CFL criterion and the CFL number should be at most equal to 0.333 to ensure the stability of the degrees of freedom.

It is noted that if only the $\mathbf{L}_i^0$ operator is used the finite element approximation is essentially a traditional finite volume scheme. Working solely on the central averages, the aforementioned spatial operator incorporated with the first-step time marching approach in Equation (14) leads to the traditional first-order upwind scheme.

3.2. Natural well-balancing in second-order

When a bed slope source term is present, the schemes must satisfy a correct balance between the source term and flux gradients (at the computational level), in order to properly reproduce stationary (or almost stationary) solutions. Following many previous researches [22, 24, 25, 28, 32], numerical method developers are particularly interested in schemes that are able to maintain the still water surface of a lake at rest ($h+z = constant$ and $q=0$) over irregular topology, where

DOI: 10.1002/fld

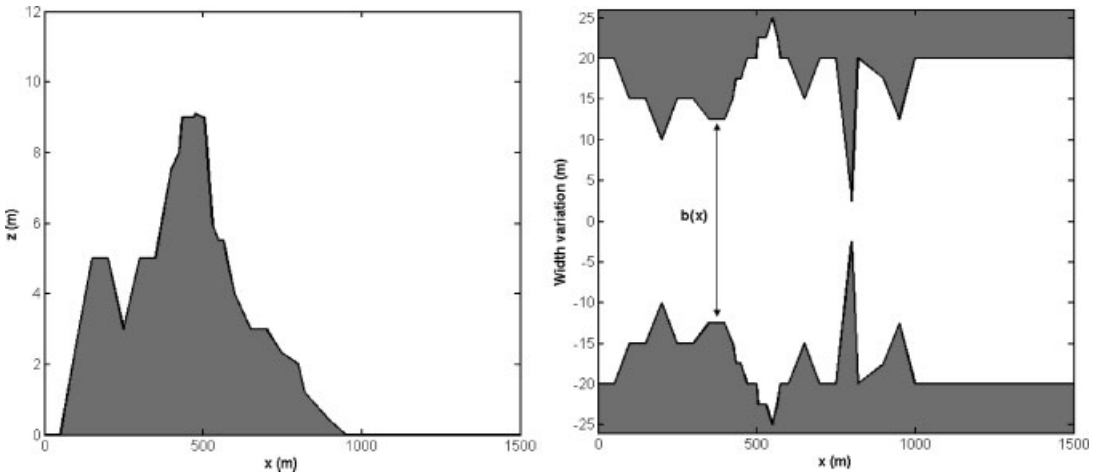

Figure 1. Schematic view of the channel geometry for the quiescent flow test.

extreme slopes are invoked (such as the complex features of the channel bed as illustrated in Figure 1 for the quiescent flow test). For this case of motionless water in a lake, the first (continuity) equation, of (1), is satisfied exactly for any consistent scheme given that the time derivative and the velocity (or discharge) terms automatically vanish. For the second (momentum) equation, part of the flux derivative term (from the LHS) and the bed slope source term (from the RHS) remain after eliminating the zero velocity terms, and the equation reduces to the hydrostatic balance of the vertical pressure gradient and gravitational force,

$$(gh^2/2)_x + ghz_x = 0 \Leftrightarrow (h+z)_x = 0 \tag{16}$$

This simplified momentum equation has to be satisfied at the discrete phase in order to construct a well-balanced scheme.

The pioneering work of Xing and Shu [37] provides an effortless basis to retain the well-balanced property in a DG environment. The well-balancing can be achieved by assuming that $\mathbf{U_h}$, which is the numerical approximation of $\mathbf{U}$, is a solution of Equation (2) with the modified source term vector $\mathbf{S}(\mathbf{U}, (S_0)_h) = [0, gh(S_0)_h]^{\mathrm{T}}$, where $(S_0)_h = -\partial z_h/\partial x$ and z_h is the $P^1(I_i)$-projection of $z(x)$ (as shown in Figure 2 for the case of quiescent flow). Following this hypothesis, the still water conditions remain locally verified ($h_h + z_h = constant$ and $q_h = 0$) and lead to a natural well balancing,

$$(gh_h^2/2)_x + gh_h(z_h)_x = 0 \Rightarrow \mathbf{F}(\mathbf{U}_h)_x = \mathbf{S}(\mathbf{U}_h, (S_0)_h) \tag{17}$$

As a result, the polynomial approximation of the channel bottom function (z_h) has to be constructed using the same generation function as that for the approximate solutions $\mathbf{U_h}$,

$$z_h(x)\rfloor_{I_i} = z_i^0 + 2z_i^1(x - x_i)/\Delta x \quad (\forall x \in I_i) \tag{18}$$

DOI: 10.1002/fld

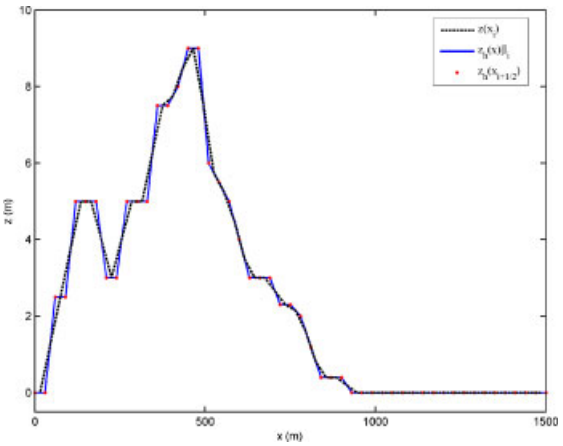

Figure 2. P^1-projection of the bed topographic function weighted against the original bed function.

The channel bottom data projection is obtained similarly as the initial condition projection of the flow vector [39]. Thus, the local average value (z_i^0) and the slope value (z_i^1) are defined by

$$z_i^0 = \frac{1}{\Delta x}\int_{x_{i-1/2}}^{x_{i+1/2}} z(x)\,\mathrm{d}x \approx \frac{1}{2}(z(x_{i+1/2}) + z(x_{i-1/2})) \tag{19}$$

$$z_i^1 = \frac{6}{\Delta x^2}\int_{x_{i-1/2}}^{x_{i+1/2}} z(x)(x - x_i)\,\mathrm{d}x \approx \frac{\sqrt{3}}{2}(z(x_i + \Delta x\sqrt{3}/6) - z(x_i - \Delta x\sqrt{3}/6)) \tag{20}$$

The corresponding bed gradient term is,

$$(S_0)_h\rfloor_{I_i} = -\frac{\mathrm{d}}{\mathrm{d}x} z_h(x)\rfloor_{I_i} = -\frac{2z_i^1}{\Delta x} \tag{21}$$

Consequently, the bed slope depends only on the local slope value z_i^1, which is reasonable and is the starting point of analysing of the natural well-balancing property of the scheme. In effect, knowing that z_i^1 is constant over I_i, and supported by Equation (20), z_i^1 should be a difference between two local z-values. To identify this local slope, a linear interpolation is performed to look at the point $z(x_i + \Delta x\sqrt{3}/6)$

$$\left(x_i + \frac{\Delta x\sqrt{3}}{6}, z\left(x_i + \frac{\Delta x\sqrt{3}}{6}\right)\right) \in [x_i; x_{i+1/2}] \times [z(x_i); z(x_{i+1/2})] \subset I_i \times [z(x_{i-1/2}); z(x_{i+1/2})] \tag{22}$$

This implies that the point belongs to the local spatial domain. The linear interpolation produces the following:

$$z\left(x_i + \frac{\Delta x\sqrt{3}}{6}\right) = \left(1 - \frac{\sqrt{3}}{3}\right) z(x_i) + \frac{\sqrt{3}}{3} z(x_{i+1/2}) \tag{23}$$

DOI: 10.1002/fld

Similarly for the second intermediate local point $z(x_i - \Delta x\sqrt{3}/6)$,

$$\left(x_i - \frac{\Delta x\sqrt{3}}{6}, z\left(x_i - \frac{\Delta x\sqrt{3}}{6}\right)\right) \in [x_{i-1/2}; x_i] \times [z(x_{i-1/2}); z(x_i)] \subset I_i \times [z(x_{i-1/2}); z(x_{i+1/2})] \quad (24)$$

and the linear interpolation produces,

$$z\left(x_i - \frac{\Delta x\sqrt{3}}{6}\right) = \left(1 - \frac{\sqrt{3}}{3}\right) z(x_i) + \frac{\sqrt{3}}{3} z(x_{i-1/2}) \quad (25)$$

Substituting Equations (23) and (25) into Equation (20), the local constant slope z_i^1 is obtained,

$$z_i^1 = \tfrac{1}{2}(z(x_{i+1/2}) - z(x_{i-1/2})) \quad (26)$$

Subsequently, the bed slope source term is obtained

$$(S_0)_h \rfloor_{I_i} = -\frac{2}{\Delta x}\left[\frac{1}{2}(z(x_{i+1/2}) - z(x_{i-1/2}))\right] = -\frac{z(x_{i+1/2}) - z(x_{i-1/2})}{\Delta x} \quad (27)$$

Equation (27) is a direct discretization of the bed slope source term, but involves only the local interfacial values of the bed function. Overall, for a second-order DG scheme (e.g. the present RKDG2 scheme) based on local linear approximation, well-balanced property is naturally gained provided that the bed slope source term is discretized by (27). However, the extension of the proposed technique to an RKDG scheme higher than second-order is not straightforward and is opened to future research.

Remark

If one considers another (traditional) way of approximating the bed slope source term,

$$S_0(x_i) = -\frac{z(x_{i+1}) - z(x_{i-1})}{2\Delta x} \quad (28)$$

which involves non-local cell-averaged values. The RKDG2 scheme is well-balanced only if the channel bottom function is uniform throughout the domain. We reconsider the two intermediate spatial points as follows:

$$\left(x_i + \frac{\Delta x\sqrt{3}}{6}, z\left(x_i + \frac{\Delta x\sqrt{3}}{6}\right)\right) \in [x_i; x_{i+1}] \times [z(x_i); z(x_{i+1})] \not\subset I_i \times [z(x_{i-1/2}); z(x_{i+1/2})] \quad (29)$$

and

$$\left(x_i - \frac{\Delta x\sqrt{3}}{6}, z\left(x_i - \frac{\Delta x\sqrt{3}}{6}\right)\right) \in [x_{i-1}; x_i] \times [z(x_{i-1}); z(x_i)] \not\subset I_i \times [z(x_{i-1/2}); z(x_{i+1/2})] \quad (30)$$

Then we again perform the linear interpolation, calculate the values $z(x_i \pm \Delta x\sqrt{3}/6)$ and substitute them back into Equation (20). This yields the following local slope value defined by non-local averages:

$$z_i^1 = \tfrac{1}{4}(z(x_{i+1}) - z(x_{i-1})) \quad (31)$$

DOI: 10.1002/fld

Table I. L^2-errors and numerical order of accuracy for Section 4.1.

	RKDG2 scheme			
	h		q	
No. of cells	L^2-errors	Order	L^2-errors	Order
25	2.9986e−004	—	3.4e−003	—
50	7.3673e−005	2.0251	8.6524e−004	1.9953
100	1.8247e−005	2.0134	2.1647e−004	1.9989
200	4.6672e−006	1.9671	5.2381e−005	2.0471
400	1.1405e−006	2.0329	1.2900e−005	2.0217
800	2.7340e−007	2.0605	3.1267e−006	2.0447

Hence, instead of Equation (27), the following bed slope term is obtained:

$$(s_0)_h\rfloor_{I_i} = -\frac{2}{\Delta x}\left[\frac{1}{4}(z(x_{i+1}) - z(x_{i-1}))\right] = S_0(x_i) \tag{32}$$

This is contradictory with the local feature of the method. According to Equations (20) and (21), z_i^1 and S_0 should be defined from the data satisfying the local linear approximation (as bed slope may not be constant across cells) to ensure the compatibility with the overall numerical scheme.

3.3. Slope limiting procedure

In the above local RKDG2 scheme, the numerical fluxes $\tilde{\mathbf{F}}_{i\pm1/2} = \tilde{\mathbf{F}}(\mathbf{U}^-_{i\pm1/2}, \mathbf{U}^+_{i\pm1/2})$ are calculated by solving the corresponding local Riemann problems using Equation (11). $\mathbf{U}^\mp_{i\pm1/2} = \mathbf{U}^0_i \pm \mathbf{U}^1_i$ are, respectively, the local limit values of the DG approximate solution at the left and right hand side of the $i+1/2$ and $i-1/2$ cell interfaces. As a result, the three-cell scheme consisting of Equations (9) and (10) is second-order accurate (Table I) and well-balanced for both water depth and flow discharge. However, along with well-balancing, the non-oscillatory property of a higher-order scheme has also to be maintained when it is applied to a problem with severe gradients flow variables, e.g. strong shock. Therefore, before solving the Riemann problem at the interface, the local approximate solution to the slope ($\mathbf{U}^1_i$) must take into account a slope limiting process to avoid the parasitical Gibbs phenomenon. In this work, a generalized *minmod* limiter is adopted to quantify the slopes for damping the numerical oscillations.

The Riemann solutions (fluxes) are estimated by inputting, to the Roe solver, the (discontinuous) slope limited approximate values ($\hat{\mathbf{U}}^-_{i\pm1/2}, \hat{\mathbf{U}}^+_{i\pm1/2}$)

$$\hat{\mathbf{U}}^\mp_{i\pm1/2} = \mathbf{U}^0_i \pm \text{minmod}(\mathbf{U}^1_i, \mathbf{U}^0_{i+1} - \mathbf{U}^0_i, \mathbf{U}^0_i - \mathbf{U}^0_{i-1}) \tag{33}$$

and

$$\text{minmod}(s_1, s_2, s_3) = \begin{cases} \text{sgn}(s_1)\min(|s_1|, |s_2|, |s_3|) & \text{if } \text{sgn}(s_1) = \text{sgn}(s_2) = \text{sgn}(s_3) \\ 0 & \text{otherwise} \end{cases} \tag{34}$$

Owing to the use of non-local average values (involving five cells), the slope limiting procedure essentially destroys the conservativity of the approximate flow variables and thus breaks the

DOI: 10.1002/fld

well-balancing property of the overall numerical scheme. This is also proved by the numerical evidence in Section 4. As suggested by Xing and Shu [37], the use of the water surface elevation instead of water depth in defining the slope limiter, to reduce the corresponding bed contribution in the limiting function, may be helpful in reducing the instability induced near the steep bed slope gradients.

4. NUMERICAL TESTS, RESULTS AND DISCUSSIONS

This section demonstrates the performance of the present local RKDG2 scheme in balancing flux and source term gradients by applying it to solve a number of steady and unsteady flow tests over varying bed geography. The effects of different slope limiting procedures (based on either water depth or surface elevation) on the well-balancing property of the scheme are also intensively investigated and discussed. The global second-order accuracy of the local RKDG2 scheme, in the presence of bed topography, is first verified. The quiescent flow test is then considered to emphasize the merit of respecting the locality property when discretizing the bed slope term. More benchmark tests are presented to stress the significance of the well-balanced property and evaluate the effects of the slope limiting procedures. $N=50$ computational cells have been chosen when simulating all the steady problems and the L^2-norm has been utilized as the convergence criterion.

4.1. Accuracy test in the presence of non-flat bottom

In this example, the second-order accuracy of the improved RKDG2 scheme is quantified by seeking numerical solutions to a generic test of shallow flow over non-flat bottom. Similar to Xing and Shu [37], the bottom function and initial conditions of the test are defined by

$$z(x)=\sin^2(\pi x) \tag{35}$$

and

$$\begin{aligned} h(x,0) &= 5+\exp[\cos(2\pi x)] \\ q(x,0) &= \sin[\cos(2\pi x)] \end{aligned} \tag{36}$$

where $x\in[0;1]$ with transmissive boundary conditions. Since the analytical solution is not available explicitly for this case, a reference solution obtained on a very fine mesh of $N=12\,800$ cells is produced and treated as an exact solution in assessing the numerical errors. Simulations are run up to $t=0.05$ s on meshes with $25, 50, 100, 200, 400$ and 800 cells. Figure 3 shows the initial flow conditions at $t=0$ and reference numerical predictions at $t=0.05$ s. Table I lists the L^2-errors evaluated for the cell averages and the order of accuracy for the proposed local RKDG2 scheme (three-cell version). It is evident that the second-order accuracy of the scheme is confirmed for both water depth and discharge in all of the simulations.

4.2. Quiescent flow test

This is a classic test, recommended by the Working Group on Dam-Break Modelling [40], for verifying the capability of a numerical scheme to handle natural topographies. The test is about a motionless flow ($h+z=12$ m and $q=0\,\mathrm{m}^2/\mathrm{s}$) occurring in a 1500 m long channel. The channel has a highly complex domain geometry and a bed topography containing positive and negative

DOI: 10.1002/fld

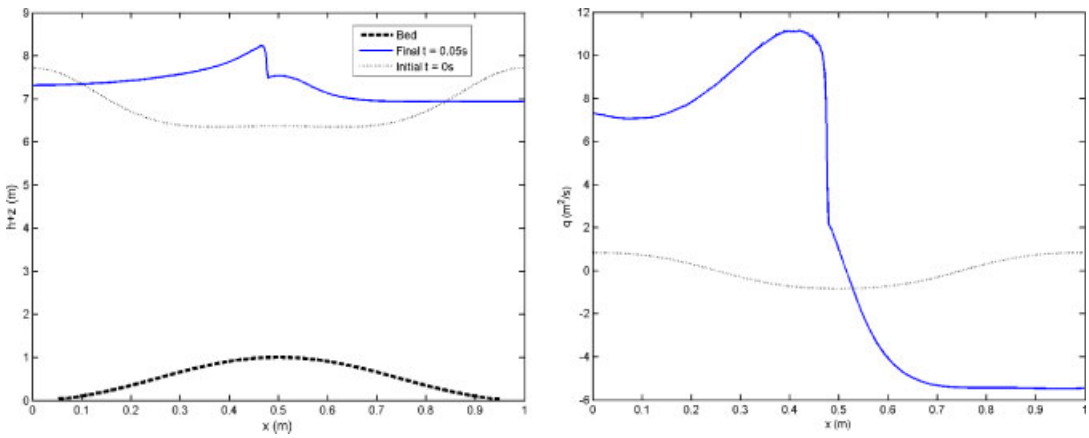

Figure 3. Initial and final solutions of water depth and discharge for the transient accuracy test.

steep slopes, as shown in Figure 1. We solve it here to testify the superior well-balancing property of the improved RKDG2 scheme. Starting from the motionless initial flow conditions and simple reflective or transmissive boundary settings, a well-balanced numerical scheme should predict a flow that preserves the horizontal water surface and zero discharge throughout a long enough simulation as no disturbance is assumed to drive the flow.

Figure 4 shows the predictions after 5000 s of simulation time, using the RKDG2 scheme associated with the non-local approximation of bed slope source term given by (28). Spurious fluxes with unacceptably large errors are generated. Figure 5 presents the results obtained by the RKDG2 scheme implemented with the local source term discretization proposed in this work. The motionless flow conditions are accurately reproduced up to the scale of round-off error (as illustrated for the discharge). The results compare favourably with those presented by Hubbard and García-Navarro [29] and Tseng [33] using different numerical schemes. However, the predictions of Hubbard and García-Navarro [29] and Tseng [33] are obtained on very fine meshes of $N = 600$ cells and $N = 500$ cells, respectively, while only 50 cells are used in the current simulation. Numerical experiments also show that, for this typical case with smooth solutions, the performance of the RKDG2 scheme is similar, regardless whether the slope limiting procedure is taken into account.

4.3. Steady smooth flow over irregular bed topography channel

The previous problem is reconsidered with a non-zero flow discharge for a more realistic situation. Tseng [33, 34] also considered this case of smooth steady flow in a channel with strong topographic variation to test several source term discretization techniques, aiming to improve a number of second-order high-resolution TVD schemes. The channel is 1500 m long and the bed topology is the same as the previous case. Because of the steady state conditions, the discharge should be constant at any cell over the computational domain. During a simulation, the downstream water depth is fixed at 15 m and the unit width discharge is specified to $0.75\,\mathrm{m}^2/\mathrm{s}$ at the upstream boundary. Figure 6 shows the numerical predictions of depth and discharge profile, after 2000 s of simulation time, produced by the RKDG2 schemes with and without implementing the limiting procedures. With regard to the depth profiles, all of the schemes generate satisfactory results when comparing with the analytical profile and no obvious difference is observed. For the flow discharge,

DOI: 10.1002/fld

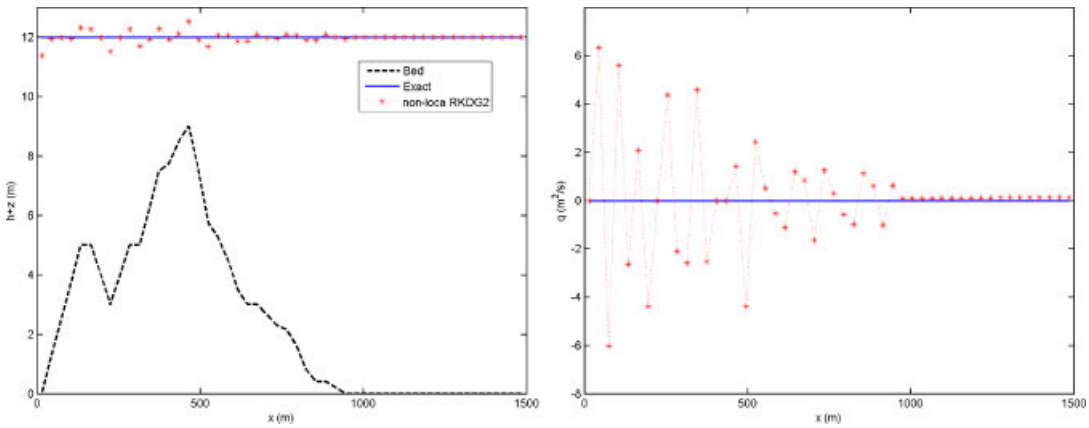

Figure 4. Comparing the exact solutions with the numerical predictions obtained by the non-local RKDG2 schemes on a grid with 50 cells.

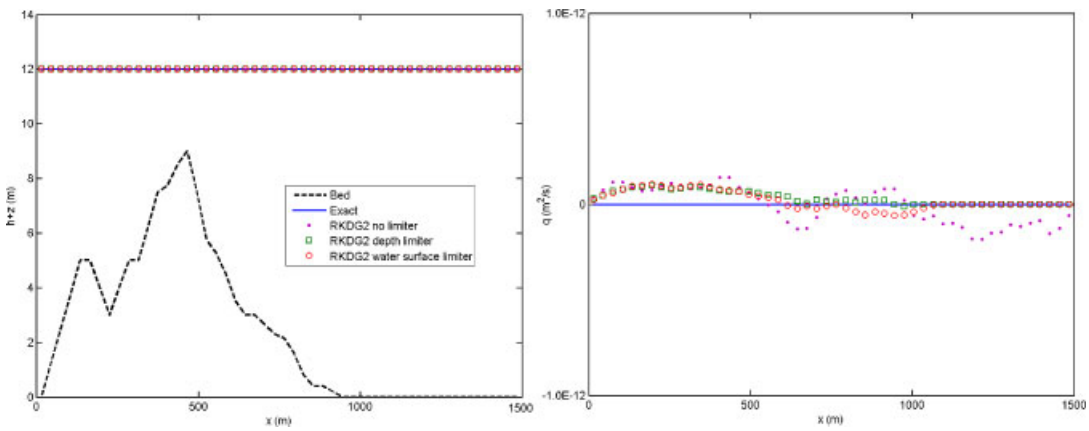

Figure 5. Comparing exact solutions with different RKDG2 predictions computed on a grid with 50 cells.

the three-cell local RKDG2 scheme without considering slope limiting reproduces perfectly the analytical solution. However, the discharge predicted by the depth slope limited RKDG2 scheme is found to deviate from the analytical solution in certain grid cells where the bed slope is steep, i.e. the numerical discharge is not conserved. This, in turn, implies that the local RKDG2 scheme provides well-balanced solutions to a flow over complex bed topography, while the scheme implemented with the water depth slope limiting procedure destroys the scheme's locality and is no longer well-balanced. However, the well-balanced property is greatly regained after using the water surface elevation to define the slope limiter.

4.4. A tidal wave flow over steps

A further informative study on the slope limiter effect is supplied in this example of a tidal wave flow over a bed with two steps (non-differentiable points), proposed at the Workshop on

DOI: 10.1002/fld

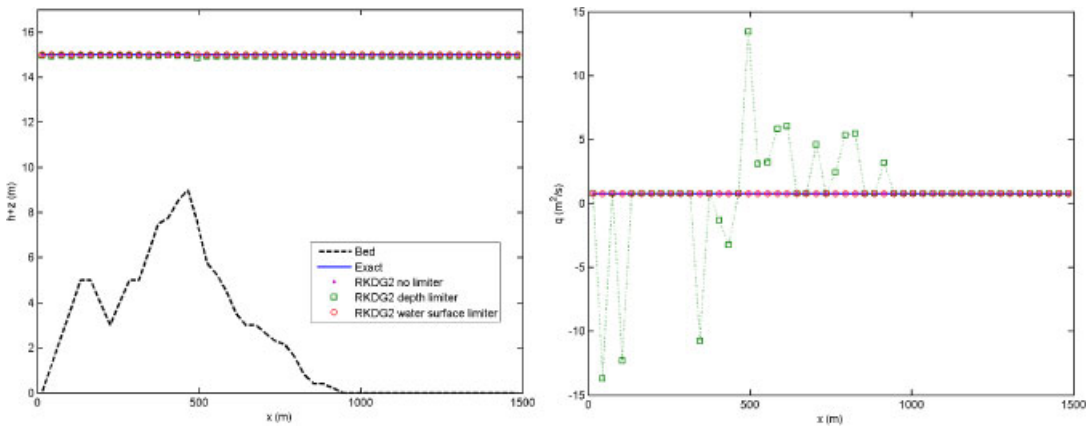

Figure 6. Steady smooth flow over irregular topography: converged numerical solutions obtained by different RKDG2 schemes.

Dam-Break Wave Simulation [40]. The flow occurs in an $L=1500\,\text{m}$ long channel with the bed profile, initial and boundary conditions, respectively, defined by,

$$z(x)=\begin{cases}8 & \text{if } |x-L/2|\leqslant L/8\\ 0 & \text{otherwise}\end{cases} \tag{37}$$

$$\begin{aligned} h(x,0) &= H(x)\\ u(x,0) &= 0\end{aligned} \tag{38}$$

$$\begin{aligned} h(0,t) &= H(0)+4-4\sin[\pi(4t/86400+1/2)]\\ u(L,t) &= 0\end{aligned} \tag{39}$$

where $H(x)=H(0)-z(x)$ with $H(0)=16\,\text{m}$. Under these conditions, the tidal wave is relatively short and an asymptotic analytical solution is derived by Bermúdez and Vázquez-Cendón [21],

$$h(x,t)=H(x)+4-4\sin[\pi(4t/86400+1/2)] \tag{40}$$

and

$$u(x,t)=\frac{(x-L)_\pi}{5400h(x,t)}\cos[\pi(4t/86400+1/2)] \tag{41}$$

Results at $t=10800$ and $32400\,\text{s}$, corresponding to the half-risen tidal flow with maximum positive velocities and to the half-ebbed tidal flow with minimum negative velocities, are compared with the asymptotic reference solutions in Figure 7. The three-cell local RKDG2 scheme and the version implemented with the surface gradient slope limiter predict fairly similar results. However, as illustrated in Figure 8, the depth gradient slope limiting RKDG2 scheme produces

DOI: 10.1002/fld

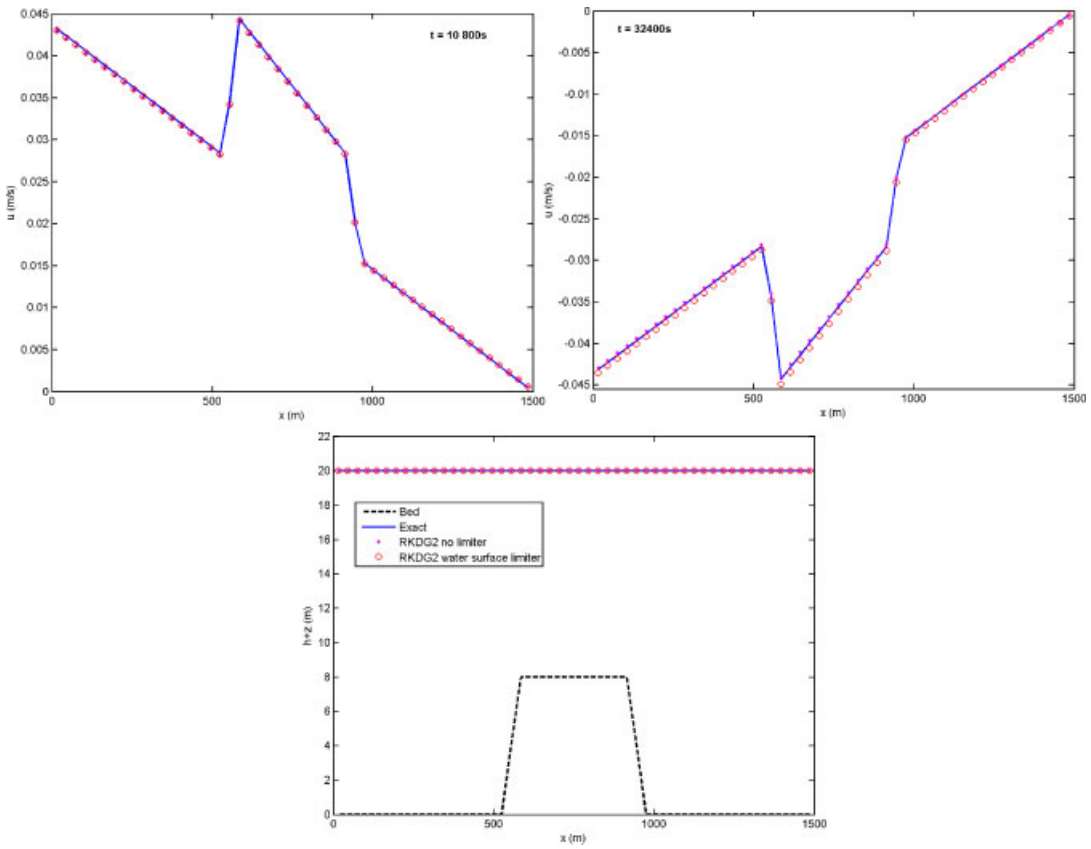

Figure 7. Tidal wave over steps: comparing the numerical predictions obtained by the local and surface gradient limited RKDG2 schemes with the asymptotic reference solutions.

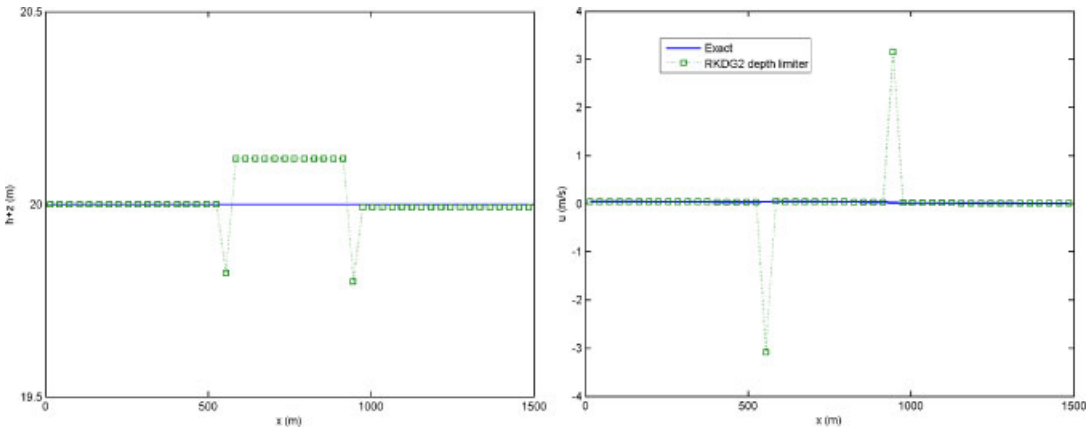

Figure 8. Tidal wave over steps: depth gradient limited RKDG2 results compared with the asymptotic reference solution.

DOI: 10.1002/fld

spiky values for both water depth and discharge in the vicinity of the non-differentiable points and the conservativity of the scheme is obviously destroyed.

4.5. *Steady flow over a hump*

This case of steady flow over a continuous but non-uniform bed topography (hump) is another classical problem recommended by the Workshop on Dam-Break Wave simulations [40], which has been widely used by many researchers to validate their well-balanced numerical schemes (e.g. Vázquez-Cendón [25]; Zhou *et al*. [31]). Different flows, e.g. subcritical, supercritical and transcritical, may be obtained by varying initial and boundary conditions [39]. Herein, only the

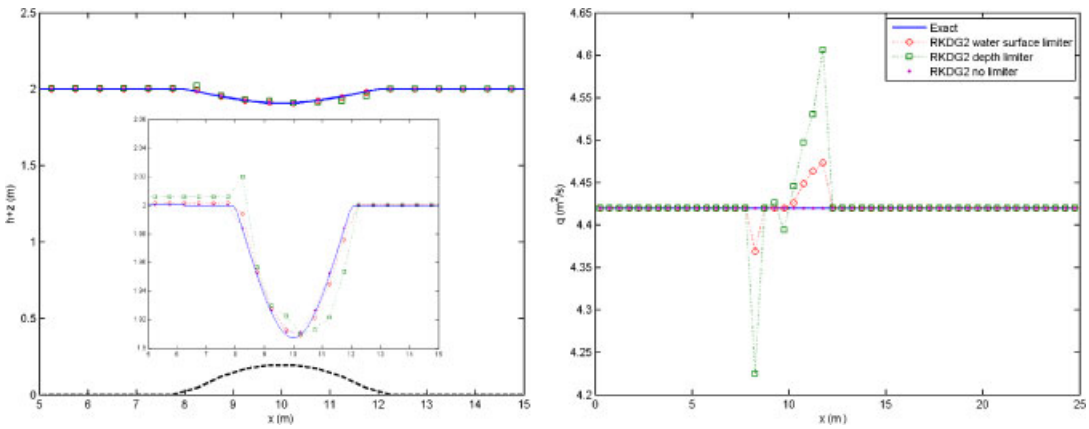

Figure 9. Steady subcritical flow over a bump: comparing numerical predictions obtained by local, depth slope limited and surface gradient slope limited RKDG2 schemes with the analytical solutions.

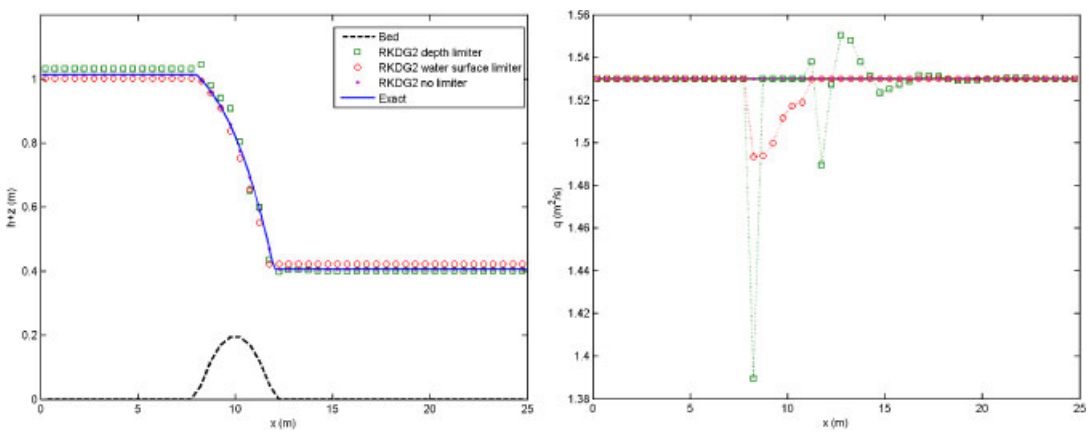

Figure 10. Steady trancritical flow over a bump: comparing numerical predictions obtained by local, depth slope limited and surface gradient slope limited RKDG2 schemes with the analytical solution.

DOI: 10.1002/fld

tests of subcritical flow and transcritical flow without a shock are considered to ensure that the non-limiting RKDG2 scheme is still applicable. The bump in a 25 m long channel is defined by,

$$z(x)=\begin{cases}0.2-0.05(x-10)^2 & \text{if } 8<x<12\\ 0 & \text{otherwise}\end{cases} \tag{42}$$

For the subcritical case, a unit width discharge of $q=4.42\,\mathrm{m}^2/\mathrm{s}$ is imposed at the upstream boundary and h is set to 2 m at the downstream end. For the case of transcritical flow without a shock, it is only necessary to fix the upstream end discharge of $q=1.53\,\mathrm{m}^2/\mathrm{s}$ (the inflow discharge and critical depth are taken as initial conditions). The analytical solutions for both tests are given by Goutal and Maurel [40].

Figures 9 and 10 compare the different steady state numerical predictions (obtained after 4162 iterations) with the analytical solutions for the tests of subcritical flow and transcritical flow, respectively. For both cases, perfect well-balanced solutions are reproduced by the local RKDG2 scheme. However, slope limiting procedures, to different extent, are observed to give numerical solutions that deviate from the analytical solutions in the regions with non-uniform bed topography. This, in turn, implies that the well-balanced property of the numerical scheme is violated. These results are not surprising because, in implementing a slope liming procedure, the physical well-balanced slope is replaced. Either the local feature of the scheme is thus destroyed in some cells, or the accuracy order is degenerated to be first-order. Between the two limiting procedures, the one using the free surface gradients provides better numerical solutions.

4.6. Dam-break over a rectangular bump

This test problem consists of discontinuous dam-break flow propagating along a channel with a rectangular hump, where the channel settings are the same as those to the tidal flow benchmark in 4.4. The initial conditions are given by two still water levels separated by a slim barrier,

$$q(x,0)=0 \quad \text{and} \quad h(x,0)=\begin{cases}20-z(x) & \text{if } x\leqslant 750\\ 15-z(x) & \text{otherwise}\end{cases} \tag{43}$$

The computations are carried out using 80 computational cells and transmissive boundary conditions are imposed in both ends of the channel. The numerical results obtained by different RKDG2 schemes are shown in Figures 11 and 12 at two different output times $t=15$ and 60 s, respectively. At $t=15$ s, the water height $h(x)$ is discontinuous at the points $x=562.5$ and 937.5 m, while the surface level $h(x)+z(x)$ is smoother. As presented in Figure 11, predictions by the three different RKDG2 schemes do not show much difference. However, as illustrated in Figure 12 for $t=60$ s, the three different RKDG2 schemes result in three distinct water surface profiles. Obviously, for this case, the local RKDG2 scheme without slope limiter provides unreliable predictions as numerical oscillations would destroy the flow solutions where severe shock appears. Supported by the previous numerical evidences where unphysical numerical, over and under, shoots in the vicinity of a step arise, the results produce by the depth gradient limited RKDG2 scheme would also be not reliable. Therefore, the surface gradient limited RKDG2 scheme is the one working well for this example (a problem involves complex topography and shock at the same time) and gives well-resolved non-oscillatory solutions.

DOI: 10.1002/fld

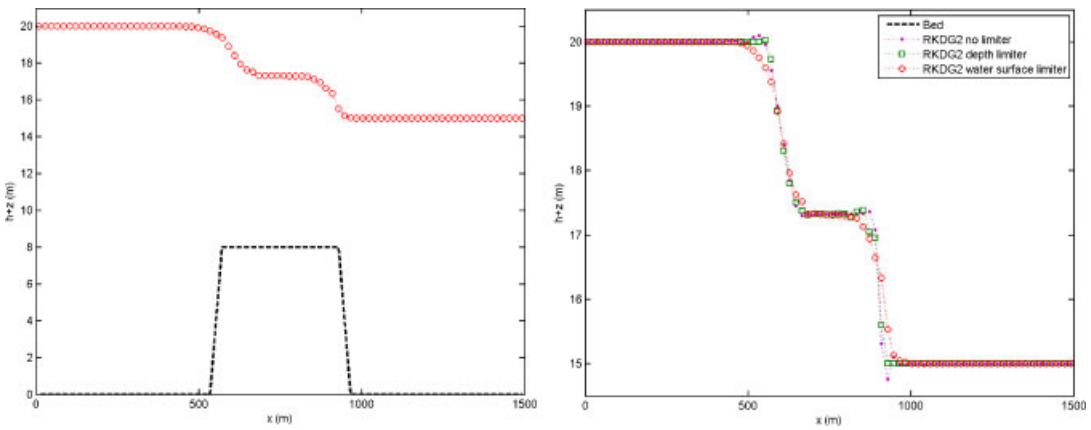

Figure 11. Transient dam-break wave propagation over steps: flow solution at $t = 15$ s (different RKDG2 predictions are compared in the zoom-in graph).

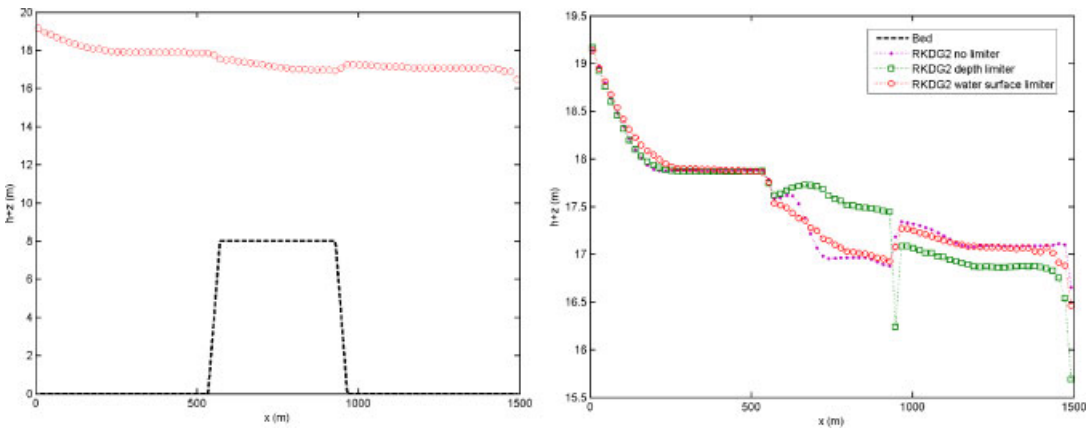

Figure 12. Transient dam-break wave propagation over steps: flow solution at $t = 60$ s (different RKDG2 predictions are compared in the zoom-in graph).

5. CONCLUSIONS

Shallow flow hydrodynamics normally occurs in domains with highly complex geometries and topographies. Therefore, when constructing a numerical model for practical shallow flow computations, e.g. river modelling, flood simulation, an important task is to accurately discretize the source terms in the governing shallow water equations to account for the effects of complicated domain features and other external forces on the flow dynamics. Compared with other source terms, (wind stress, Coriolis effect, friction force, etc.), handling the bed slope term has been accepted as a more challenging computational issue.

This paper has attempted to provide some insights into this problem in the context of constructing a DG scheme for solving the Saint Venant equations. An RKDG2 numerical scheme [39] is first

DOI: 10.1002/fld

introduced where a simple approach based on the linear polynomial projection of the bottom topographic function is used to discretize the bed slope source term. The proposed RKDG2 scheme is constructed on a three-cell stencil, i.e. only the local flow information is required. This local feature gives rise to a natural well-balanced numerical scheme that exactly satisfies the C-property and provides conserved solutions for both free surface elevation and discharge. The outstanding well-balanced property of the present local RKDG2 scheme is intensively tested by applying to shallow flow benchmarks involving complex bed profiles.

However, when applying to simulate a flow with steep gradients, a second- or higher-order numerical scheme is known to predict unphysical oscillations in the vicinity of the flow discontinuity. Without any numerical implementation to avoid these spurious oscillations, the three-cell local RKDG2 scheme may not be applicable to simulate more complex flow phenomena involving shock-type flow discontinuity, despite its important advantages in well-balancing. Nowadays, a well-established way to deal with this is to implement a slope limiting procedure. In order to construct a slope-limited RKDG2 scheme, it is necessary to at least involve flow information from five cells. The effects of two different slope limiting functions, defined based on either water depth or surface gradient, on the flow solutions are then discussed in the context of numerical tests. It is found that the absolute well-balancing property of the local RKDG2 scheme is destroyed to some extent after incorporating a slope limiting procedure due to the violation of the scheme's locality. Comparing with the water depth limiting procedure, the surface elevation-based slope limiting procedure can retain most of the well-balancing property and leads to better solutions. Therefore, when applying to complex flow problems, e.g. dam-break simulations, a surface gradient limited RKDG2 scheme may provide an optimum way to give well-balanced and oscillation-free solutions.

In summary, this work discusses the important issues related to constructing a well-balanced RKDG2 scheme for solving shallow water equations, which should be taken into account in practical flow simulations.

ACKNOWLEDGEMENTS

This work is funded by the U.K. Engineering and Physical Sciences Research Council (EPSRC) through grant: EP/F030177/1. The first author thanks Prof. Vincent Guinot from the University of Montpellier for several inspiring ideas.

REFERENCES

1. Guinot V. *Godunov-type Schemes*: *An Introduction for Engineers*. Elsevier: Amsterdam, 2003.
2. Hirsch C. *Numerical Computation of Internal and External Flows*, *Computational Methods for Inviscid and Viscous Flows*. Wiley: Chichester, England, New York, 1990.
3. Liang Q, Borthwick AGL. Adaptive quadtree simulation of shallow flows with wet–dry fronts over complex topography. *Computers and Fluids* 2009; **38**(2):221–234.
4. Schwanenberg D. Die Runge–Kutta-discontinuous-Galerkin-Methode zur Lösung konvektionsdominierter tiefengemittelter Flachwasserprobleme. *Ph.D. Thesis*, Fakultät für Bauingenieurwesen, 2003.
5. Toro EF. *Shock-capturing Methods for Free-surface Shallow Flows*. Wiley: New York, 2001.
6. Toro EF, García-Navarro P. Godunov-type methods for free-surface shallow flows: a review. *Journal of Hydraulic Research* 2007; **45**(6):737–751.
7. Lhomme J, Guinot V. A general approximate-state Riemann solver for hyperbolic systems of conservation laws with source terms. *International Journal for Numerical Methods in Fluids* 2007; **55**(9):1509–1540.

DOI: 10.1002/fld

8. Kesserwani G, Mosé R, Vazquez J, Ghenaim A. A practical implementation of high-order RKDG models for the 1D open-channel flow equations. *International Journal for Numerical Methods in Fluids* 2009; DOI: 10.1002/fld.1879.
9. Shu CW, Osher S. Efficient implementation of essentially non-oscillatory shock capturing schemes. *Journal of Computational Physics* 1988; **77**(2):439–471.
10. Cockburn B, Shu CW. Runge–Kutta discontinuous Galerkin methods for convection-dominated problems. *Journal of Scientific Computing* 2001; **16**(3):173–261.
11. Cockburn B, Lin S, Shu CW. TVB Runge–Kutta local projection discontinuous Galerkin finite element method for conservation laws III: one dimensional systems. *Journal of Computational Physics* 1989; **84**(1):90–113.
12. Cockburn B, Shu CW. The Runge–Kutta local projection P1-discontinuous Galerkin method for scalar conservation laws. *ESAIM*: *Mathematical Modelling and Numerical Analysis* 1991; **25**(3):337–361.
13. Cockburn B, Shu CW. TVB Runge–Kutta local projection discontinuous Galerkin finite element method for scalar conservation laws II: general framework. *Mathematics of Computation* 1989; **52**(186):411–435.
14. Cockburn B. Discontinuous Galerkin methods. *Zeitschrift für Angewandte Mathematik und Mechanik* 2003; **83**(11):731–754.
15. Kurganov A, Petrova G. A second-order well-balanced positivity preserving central-upwind scheme for the Saint-Venant system. *Communications in Mathematical Sciences* 2007; **5**(1):133–160.
16. LeVeque RJ. Balancing source terms and flux gradients in high resolution Godunov methods. *Journal of Computational Physics* 1998; **146**(1):346–365.
17. Mohammadian A, Le Roux DY. Simulation of shallow flows over variable topographies using unstructured grids. *International Journal for Numerical Methods in Fluids* 2006; **52**(5):473–498.
18. Noelle S, Pankratz N, Puppo G, Natvig JR. Well-balanced finite volume schemes of arbitrary order of accuracy for shallow water flows. *Journal of Computational Physics* 2006; **213**(2):474–499.
19. Vukovic S, Sopta L. ENO and WENO schemes with the exact conservation property for one-dimensional shallow water equations. *Journal of Computational Physics* 2002; **179**(2):593–621.
20. Roe PL. Upwind differencing schemes for hyperbolic conservation laws with source terms. In *Proceedings of Nonlinear Hyperbolic Problems*, Carasso C, Raviart P, Serre D (eds). Lecture Notes in Mathematics, vol. 1270. Springer: Berlin, 1986; 41–51.
21. Bermúdez A, Vázquez-Cendón ME. Upwind methods for hyperbolic conservation laws with source terms. *Computers and Fluids* 1994; **23**(8):1049–1071.
22. Črnjarić-Žic N, Vuković S, Sopta L. Balanced finite volume WENO and central WENO schemes for the shallow water and the open-channel flow equations. *Journal of Computational Physics* 2004; **200**(2):512–548.
23. Crossley AJ, Wright NG. Time accurate local time stepping for the unsteady shallow water equations. *International Journal for Numerical Methods in Fluids* 2005; **48**(7):775–799.
24. García-Navarro P, Vázquez-Cendón ME. On numerical treatment of the source terms in shallow water equations. *Computers and Fluids* 2000; **29**(8):951–979.
25. Vázquez-Cendón ME. Improved treatment of source terms in upwind schemes for the shallow water equations in channels with irregular geometry. *Journal of Computational Physics* 1999; **148**(2):497–526.
26. Greenberg JM, LeRoux AY. A well-balanced scheme for numerical processing of source terms in hyperbolic equations. *SIAM Journal on Numerical Analysis* 1996; **33**(1):1–16.
27. Audusse E, Bouchut F, Bristeau MO, Klein R, Perthame B. A fast and stable well-balanced scheme with hydrostatic reconstruction for shallow water flows. *SIAM Journal on Scientific Computing* 2004; **25**(6):2050–2065.
28. Aureli F, Maranzoni A, Mignosa P, Ziveri C. A weighted surface-depth gradient method for the numerical integration of the 2D shallow water equations with topography. *Advances in Water Resources* 2008; **31**(7):962–974.
29. Hubbard ME, García-Navarro P. Flux difference splitting and the balancing of source terms and flux gradients. *Journal of Computational Physics* 2000; **65**(1):89–125.
30. Zhou JG, Causon DM, Ingram DM, Mingham CG. Numerical solutions of the shallow water equations with discontinuous bed topography. *International Journal for Numerical Methods in Fluids* 2002; **38**(8):769–788.
31. Zhou JG, Causon DM, Ingram DM, Mingham CG. The surface gradient method for the treatment of source terms in the shallow-water equations. *Journal of Computational Physics* 2001; **168**(1):1–25.
32. Rogers BD, Borthwick AGL, Taylor PH. Mathematical balancing of flux gradient and source terms prior to using Roe's approximate Riemann solver. *Journal of Computational Physics* 2003; **192**(2):422–451.
33. Tseng MH. *Improved Treatment of Source Terms in TVD Scheme for Shallow Water Equations*. *Advances in Water Resources* 2004; **27**(6):617–629.
34. Tseng MH. The improved surface gradient method for flows simulation in variable bed topography channel using TVD-MacCormack scheme. *International Journal for Numerical Methods in Fluids* 2003; **43**(1):71–91.

35. Caleffi V, Valiani A, Bernini A. Fourth-order balanced source term treatment in central WENO schemes for shallow water equations. *Journal of Computational Physics* 2006; **218**(1):228–245.
36. Xing Y, Shu CW. High order well-balanced finite volume WENO schemes and discontinuous Galerkin methods for a class of hyperbolic systems with source terms. *Journal of Computational Physics* 2006; **214**(2):567–598.
37. Xing Y, Shu CW. A new approach of high order well-balanced finite volume WENO schemes and discontinuous Galerkin methods for a class of hyperbolic systems with source terms. *Communications in Computational Physics* 2006; **1**(1):101–135.
38. Kesserwani G, Ghostine R, Vazquez J, Ghenaim A, Mosé R. Riemann solvers with Runge–Kutta discontinuous Galerkin schemes for the 1D shallow water equations. *Journal of Hydraulic Engineering* (ASCE) 2008; **134**(2):243–255.
39. Kesserwani G, Ghostine R, Vazquez J, Ghenaim A, Mosé R. Application of a second order Runge–Kutta discontinuous Galerkin scheme for the shallow water equations with source terms. *International Journal for Numerical Methods in Fluids* 2008; **56**(7):805–821.
40. Goutal N, Maurel F. *Proceedings of the 2nd Workshop on Dam Break Wave Simulation*, *Technical Report IIE-13/97/016A*, Electricité de France, Département Laboratoire National d'Hydraulique, Groupe Hydraulique Fluviale, 1997.

DOI: 10.1002/fld